

High-Temperature Modeling of Transport Properties in Hypersonic Flows

Daniel Dias Loureiro

Aerospace Engineering
Instituto Superior Técnico

19 Nov 2015



Hypersonic Reentry Flows



Artist rendering, credit: Dassault Aviation

esa's IXV

Intermediate eXperimental Vehicle
Reentering at 7700 m/s, Feb. 2015

Blunt bodies, $Ma = 20$ to 50 :

- Detached bow shock
 - Extreme deceleration
- High temperature gas
 - Chemically reacting
 - Partially ionized (plasma)
- Electrically charged flow
 - Loss of telemetry (Blackout)
- Radiative and **convective heating**
 - Thermal protection system

1 Introduction

2 Physical Models

- Chemical and Thermal Non-equilibrium
- Governing of equations
- Transport Models

3 Results

- Verification & Validation
- Application: RAM-C II

4 Conclusions

1 Introduction

2 Physical Models

- Chemical and Thermal Non-equilibrium
- Governing of equations
- Transport Models

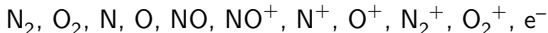
3 Results

- Verification & Validation
- Application: RAM-C II

4 Conclusions

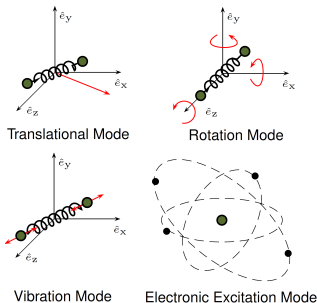
Chemical Non-Equilibrium

- Chemical Kinetic timescales \approx Flow timescales,
 - composition of the flow-field is determined as part of the simulation procedure.
- Earth atmosphere is described as a mixture of 11 chemical species:



Thermal Non-Equilibrium

- Molecules and atoms can store energy in various modes (degrees of freedom).
- In low density conditions, energy exchanges between modes may be slow relative to flow velocity.
- The flow is characterized by multiple temperatures T_k .



Conservation Equations

- **Mass of species s :**

$$\frac{\partial}{\partial t} (\rho c_s) + \vec{\nabla} \cdot (\rho \vec{u} c_s) = \vec{\nabla} \cdot \vec{J}_s + \dot{\omega}_s$$

- **Momentum:**

$$\frac{\partial}{\partial t} (\rho \vec{u}) + \vec{\nabla} \cdot (\rho \vec{u} \otimes \vec{u}) = \vec{\nabla} \cdot [\tau] - \vec{\nabla} P$$

- **Total energy:**

$$\frac{\partial}{\partial t} (\rho E) + \vec{\nabla} \cdot (\rho \vec{u} E) = \vec{\nabla} \cdot \left(\sum_k \vec{q} \vec{C}_k + \sum_s \vec{J}_s h_s + \vec{u} \cdot [\tau] - P \vec{u} \right)$$

- **Non-equilibrium energy k :**

$$\frac{\partial}{\partial t} (\rho \varepsilon_k) + \vec{\nabla} \cdot (\rho \vec{u} h_k) = \vec{\nabla} \cdot \left(\vec{q} \vec{C}_k + \sum_s \vec{J}_s h_{s,k} \right) + \dot{\Omega}_k$$

SPARK Aerothermodynamics code:

- Multi-Species, Multi-Temperature
- Finite Volumes Method
- Multi-block structured mesh
- Thermo-chemical database
- Modular and object oriented, programed in Fortran 2008

Conservation Equations

- **Mass of species s :**

$$\frac{\partial}{\partial t} (\rho c_s) + \vec{\nabla} \cdot (\rho \vec{u} c_s) = \vec{\nabla} \cdot \vec{J}_s + \dot{\omega}_s$$

- **Momentum:**

$$\frac{\partial}{\partial t} (\rho \vec{u}) + \vec{\nabla} \cdot (\rho \vec{u} \otimes \vec{u}) = \vec{\nabla} \cdot [\tau] - \vec{\nabla} P$$

- **Total energy:**

$$\frac{\partial}{\partial t} (\rho E) + \vec{\nabla} \cdot (\rho \vec{u} E) = \vec{\nabla} \cdot \left(\sum_k \vec{q} \vec{C}_k + \sum_s \vec{J}_s h_s + \vec{u} \cdot [\tau] - P \vec{u} \right)$$

- **Non-equilibrium energy k :**

$$\frac{\partial}{\partial t} (\rho \varepsilon_k) + \vec{\nabla} \cdot (\rho \vec{u} h_k) = \vec{\nabla} \cdot \left(\vec{q} \vec{C}_k + \sum_s \vec{J}_s h_{s,k} \right) + \dot{\Omega}_k$$

SPARK Aerothermodynamics code:

- Multi-Species, Multi-Temperature
- Finite Volumes Method
- Multi-block structured mesh
- Thermo-chemical database
- Modular and object oriented, programmed in Fortran 2008

This work provides models to compute the **dissipative terms**

Dissipative fluxes

- The **mass diffusion flux** \vec{J}_s is modeled by Fick's Law of diffusion, for each species s relative to the mixture:

$$\vec{J}_s = \rho D_s \vec{\nabla}(c_s)$$

- The **viscous stress tensor** $[\tau]$ assumes a Newtonian fluid and Stokes hypothesis:

$$[\tau] = \mu \left(\vec{\nabla} \vec{u} + (\vec{\nabla} \vec{u})^\top \right) - \frac{3}{2} \mu (\vec{\nabla} \cdot \vec{u}) [\mathbf{I}]$$

- The **conduction heat flux** \vec{q}_{C_k} is given by Fourier's Law, for each non-equilibrium temperature T_k :

$$\vec{q}_{C_k} = \lambda_k \vec{\nabla} T_k$$

Transport Coefficients

Mass Diffusion D_s

Viscosity μ

Thermal Conductivity λ_k

- Consequence of the interactions between particles at microscopic level.
- Functions of temperature and local chemical composition, requiring computation in real-time.
- Exact solutions computationally expensive → **Approximate methods**

Wilke/Blottner/Eucken Model

Blottner Model

Viscosity μ_s determined for each species s , using curve fits as function of T

$$\mu_s = 0.1 \exp((A_s \ln T + B_s) \ln T + C_s)$$

Eucken Relation

Thermal conductivity $\lambda_{k,s}$ given by μ_s and specific heat $C_{V k,s}$, per species s and energy mode k

$$\lambda_{k,s} = \begin{cases} \frac{5}{2} \mu_s C_{V \text{tra},s} & \text{if } k=\text{tra} \\ \mu_s C_{V k,s} & \text{if } k=\text{rot,vib,exc} \end{cases}$$

Wilke Mixing Rule

Global viscosity μ and thermal conductivities λ_k are averaged according to gas composition x_s

$$\mu = \sum_s \frac{x_s \mu_s}{\phi_s} \quad \text{and} \quad \lambda_k = \sum_s \frac{x_s \lambda_{k,s}}{\phi_s} \quad \text{with:}$$

$$\phi_s = \sum_r x_r \left[1 + \left(\frac{\mu_s}{\mu_r} \right)^{1/2} \left(\frac{M_r}{M_s} \right)^{1/4} \right]^2 \left[8 \left(1 + \frac{M_s}{M_r} \right) \right]^{-1/2}$$

Constant Lewis Number

Diffusion coefficient D_s assumes a constant Lewis number (same for all species)

$$D_s = D = \frac{\text{Le} \lambda}{\rho C_P} \quad \text{with} \quad \text{Le} = 1.2$$

Gupta-Yos/CCS Model

Collision Cross-Section

Cross-section areas $\pi\bar{\Omega}_{sr}^{(l,l)}$, are defined by curve fits as function of T for each pair of chemical species (s, r combinations)

$$\pi\bar{\Omega}_{sr}^{(l,l)} = D_{\bar{\Omega}_{sr}^{(l,l)}} T \left[A_{\bar{\Omega}_{sr}^{(l,l)}} (\ln T)^2 + B_{\bar{\Omega}_{sr}^{(l,l)}} \ln T + C_{\bar{\Omega}_{sr}^{(l,l)}} \right]$$

$$\Delta_{sr}^{(l)} = \frac{8}{3} \left[\frac{2M_s M_r}{\pi R_u T_c (M_s + M_r)} \right]^{1/2} \pi\bar{\Omega}_{sr}^{(l,l)} \quad \text{with } l=\{1,2\}$$

Gupta-Yos Mixing Rule

Global viscosity μ and thermal conductivities λ_k are averaged according to gas composition x_s

$$\mu = \sum_s \frac{x_s m_s}{\sum_r x_r \Delta_{sr}^{(2)}}$$

$$\lambda_{\text{tra}} = \frac{5}{2} \sum_s \frac{x_s m_s C_{V\text{tra},s}}{\sum_r \alpha_{sr} x_r \Delta_{sr}^{(2)}}$$

$$\lambda_{k \neq \text{tra}} = \sum_s \frac{x_s m_s C_{V k,s}}{\sum_r x_r \Delta_{sr}^{(1)}}$$

Effective diffusion

The diffusion coefficient of each chemical species relative to the mixture D_s is averaged from the binary diffusion coefficients D_{sr}

$$D_{sr} = \frac{k_B T_c}{P \Delta_{sr}^{(1)}} \quad \rightarrow \quad D_s = \frac{1 - x_s}{\sum_{r \neq s} \frac{x_r}{D_{sr}}}$$

Diffusion Flux

- Generalized Fick Law: $\vec{J}_s^* = \rho D_s \vec{\nabla}(c_s)$

Mass Conservation

Due to approximations, the total diffusion flux violates the mass conservation condition

$$\sum \vec{J}_s = \vec{\epsilon} \neq 0$$

Ambipolar Effect

Due to charge interaction, ions and electrons have similar diffusion velocities.
Can be introduced by ensuring neutral flux:

$$\sum q_s \vec{J}_s = 0$$

and correcting the ion diffusion coefficient:

$$D_{\text{ion}}^a = \left(1 + \frac{T_e}{T_{\text{ion}}}\right) D_{\text{ion}}$$

Flux Correction

An improved normalization method was implemented that ensures both conditions:

$$\vec{\epsilon} = \frac{\sum_{s \neq e} \vec{J}_s^* + \sum_{s=\text{ion}} \frac{M_e}{M_s} \vec{J}_s^*}{1 + \sum_{s=\text{ion}} \frac{M_e}{M_s} \frac{c_s}{1 - c_e}}$$

$$\vec{J}_{s \neq e} = \vec{J}_s^* - \frac{c_s}{1 - c_e} \vec{\epsilon}$$

$$\vec{J}_e = M_e \sum_{s=\text{ion}} \frac{1}{M_s} \vec{J}_s$$

1 Introduction

2 Physical Models

- Chemical and Thermal Non-equilibrium
- Governing of equations
- Transport Models

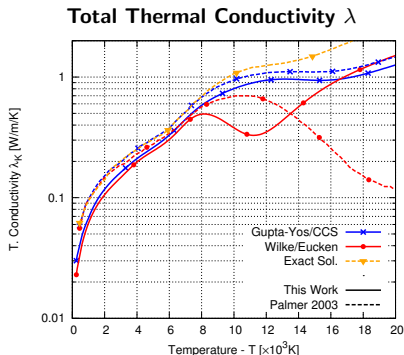
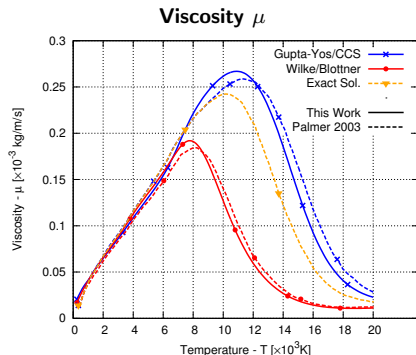
3 Results

- Verification & Validation
- Application: RAM-C II

4 Conclusions

Verification & Validation

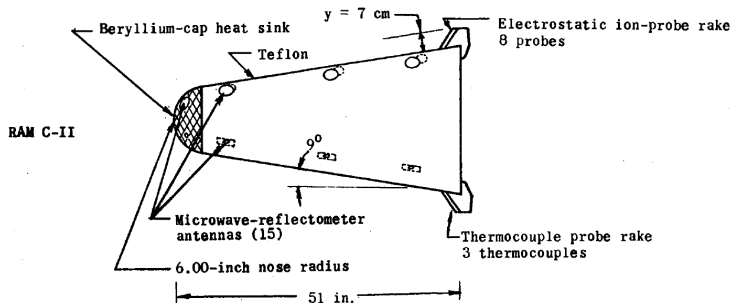
Results for the equilibrium composition of Air (11 species) at $P = 1$ atm



- Good correlation with previous work. Discrepancies due to different input data.
- Both models are valid only at low temperatures (weakly ionized gas).
- Gupta-Yos/CCS model is accurate for a larger temperature range.
- Wilke/Blottner/Eucken model is 50% faster to compute.

Application: RAM-C II Experiment

Experiments in the late 1960's for studying communications blackout, measured the electron density in the plasma around a blunt capsule, as it reenters earth atmosphere.

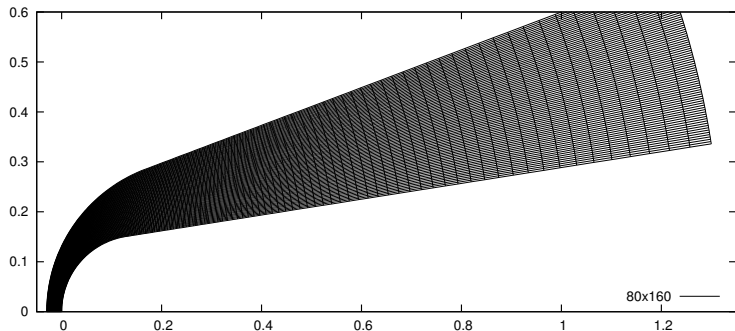
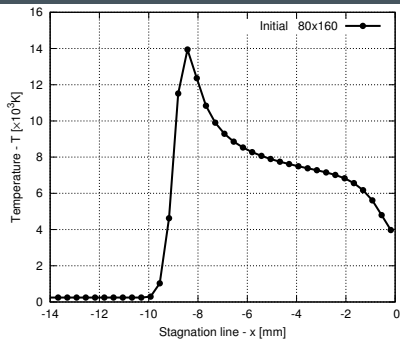


- The conditions at 61 km altitude, $Ma = 24$, have been simulated.

Computational Mesh

Axisymmetric Flow \rightarrow 2D Mesh

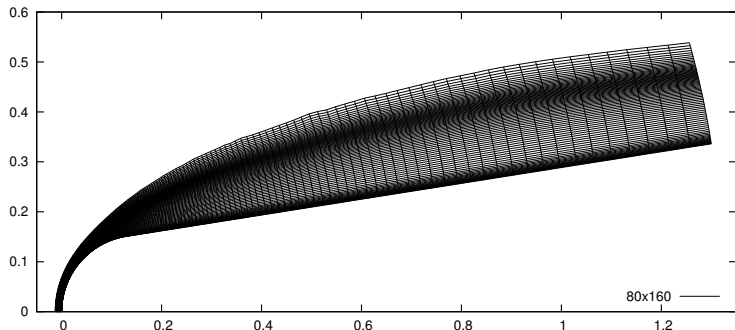
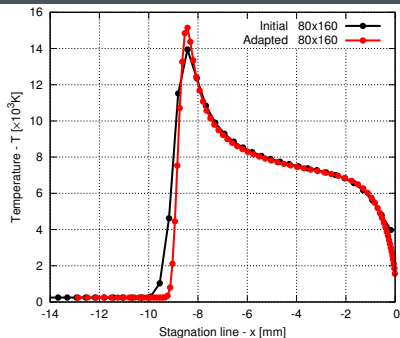
- 1 Initial Uniform Mesh 80×160 cells



Computational Mesh

Axisymmetric Flow \rightarrow 2D Mesh

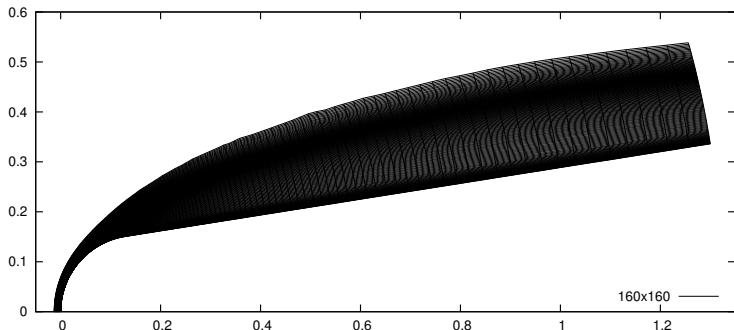
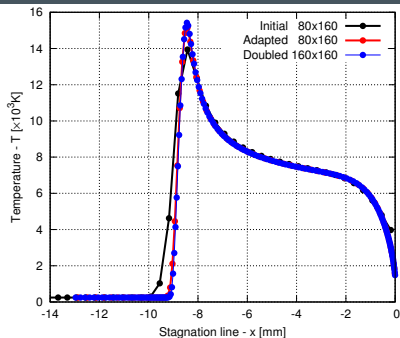
- 1 Initial Uniform Mesh 80×160 cells
- 2 Clustering at Shock and Wall



Computational Mesh

Axisymmetric Flow \rightarrow 2D Mesh

- 1 Initial Uniform Mesh 80×160 cells
- 2 Clustering at Shock and Wall
- 3 Doubling for convergence check

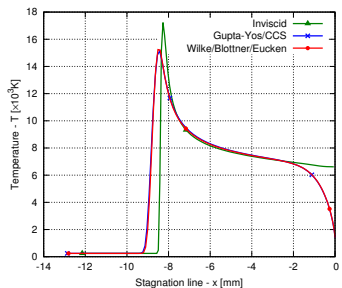
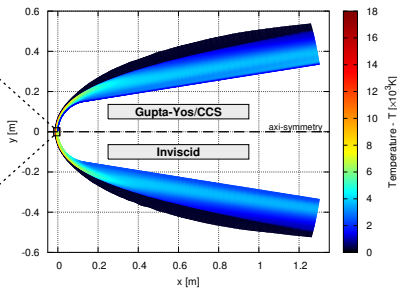
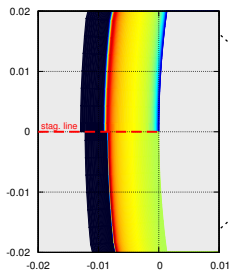


Temperature

Thermal equilibrium

RAM-C II
 $T_{\infty} = 244 \text{ K}$
 $T_{\text{wall}} = 1200 \text{ K}$

$h = 61 \text{ km}$
 $P_{\infty} = 19.3 \text{ Pa}$
 $V_{\infty} = 7650 \text{ m/s}$
 (BC: Isothermal, Non-Catalytic)



- When transport processes (dissipation) are considered:
 - Peak temperature 13% lower.
 - Significant improvement in behavior at the wall.
 - Better solver stability.
- Difference between the two transport models is negligible.

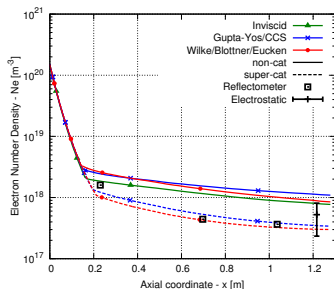
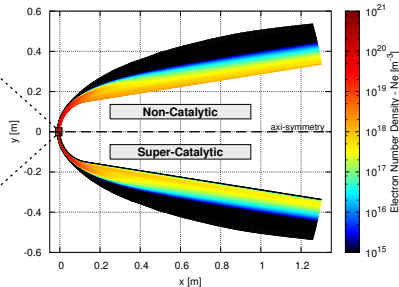
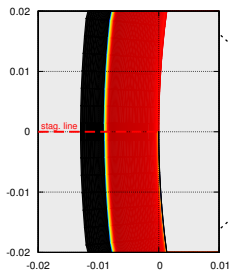
Electron Density (experiment results)

Thermal equilibrium, catalytic effect

RAM-C II
 $T_{\infty} = 244 \text{ K}$
 $T_{\text{wall}} = 1200 \text{ K}$

$h = 61 \text{ km}$
 $P_{\infty} = 19.3 \text{ Pa}$
 (BC: Isothermal)

$Ma = 24$
 $V_{\infty} = 7650 \text{ m/s}$



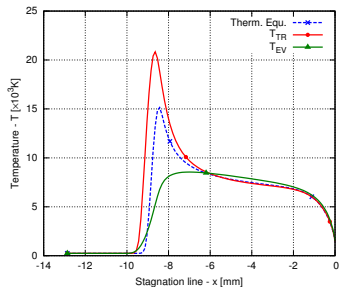
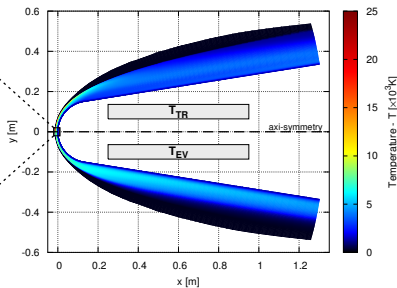
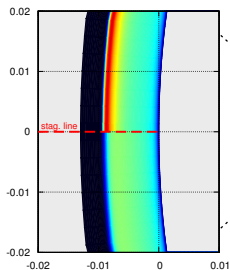
- Wall catalicity condition has a significant effect.
- Excellent agreement of the results with experimental data, when total ion recombination at the wall is considered.
- The influence of the transport model is negligible.

Thermal Non-Equilibrium

Two temperature model: T_{TR} , T_{EV}

RAM-C II
 $T_{\infty} = 244 \text{ K}$
 $T_{\text{wall}} = 1200 \text{ K}$

$h = 61 \text{ km}$
 $P_{\infty} = 19.3 \text{ Pa}$
 $V_{\infty} = 7650 \text{ m/s}$
 (BC: Isothermal, Non-Catalytic)



- The non-equilibrium effect is very strong with 40% difference of T_{TR} relative to equilibrium, and 60% between T_{TR} and T_{EV} .
- Causes increase in shock thickness and standoff distance.
- Correlation with experimental results for electron density not significantly affected.

Wall Heat Flux

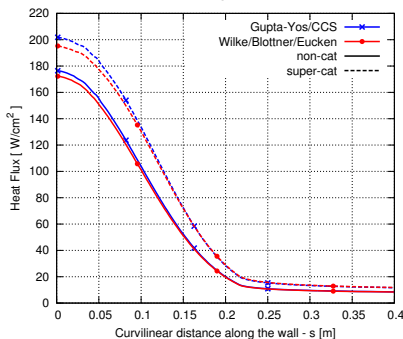
RAM-C II

 $T_{\infty} = 244 \text{ K}$ $T_{\text{wall}} = 1200 \text{ K}$ $h = 61 \text{ km}$ $P_{\infty} = 19.3 \text{ Pa}$

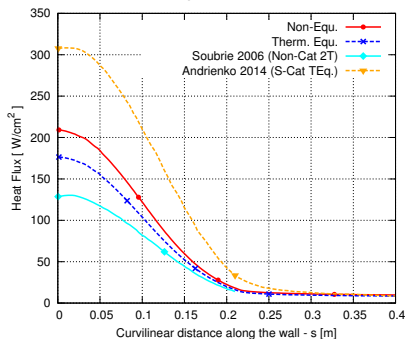
(BC: Isothermal)

 $Ma = 24$ $V_{\infty} = 7650 \text{ m/s}$

Thermal Equilibrium



Thermal Non-Equilibrium - T_{TR} , T_{EV}



- Negligible effect of the transport model (2%).
- Significant influence of wall catalicity (14%).
- Significant effect of thermal non-equilibrium (19%).
- Within the range of predictions found on previous works.

Conclusions

- Two transport models were successfully implemented with flexibility for any multi-temperature model. Improvements introduced in charged particle diffusion.
- Implementation validated against previous works and experimental data in an application case. Both models are well suited for the case tested, although the Gupta-Yos/CCS model is known to be more accurate for higher entry velocities.
- New capabilities added to the SPARK code, such as the computation of the heat flux at the wall.

Conclusions

- Two transport models were successfully implemented with flexibility for any multi-temperature model. Improvements introduced in charged particle diffusion.
- Implementation validated against previous works and experimental data in an application case. Both models are well suited for the case tested, although the Gupta-Yos/CCS model is known to be more accurate for higher entry velocities.
- New capabilities added to the SPARK code, such as the computation of the heat flux at the wall.

Future Works:

- Additional V&V should be performed for other multi-temperature and chemical models, and also on different flow conditions.
- Update the collision cross section and viscosity database for Air, and complement data with additional chemical species – different planetary atmospheres.
- Extend the transport modeling for use with state-to-state chemistry.

Thank you!

Questions?

Suggestions?